Effect of axial magnetic field variations on asymmetry-induced transport in a non-neutral plasma trap

D. L. Eggleston and K. J. McMurtry
Occidental College, Physics Department, Los Angeles, California 90041

A. A. Kabantsev and C. F. Driscoll
Physics Department, University of California, San Diego, California 92093

(Received 22 November 2005; accepted 25 January 2006; published online 10 March 2006)

It has been suggested that magnetically trapped particles play a role in the asymmetry-induced radial transport observed in the Occidental non-neutral plasma trap. This magnetic trapping would occur due to a small increase ($\beta \equiv \delta B/B \approx 0.4\%$) in magnetic field at the center of our solenoid and would keep low velocity particles confined to the ends of the trap. To test this suggestion, three coils of additional windings have been added to the trap solenoid thus allowing adjustment of the axial field variation δB. The effect of these adjustments on typical radial flux resonances is investigated. Making B as uniform as possible reduces β by a factor of 5.9, but this produces little change in the transport. Varying β over the broader range from −8.5% to 9.5% gives variations of 20%–90% in the magnitude, peak frequency, and width of the flux resonances, but these variations do not match the predictions of a simple model of trapped particle transport based on isotropic particle distributions. © *2006 American Institute of Physics*. [DOI: 10.1063/1.2177607]

I. INTRODUCTION

The long confinement time of non-neutral plasmas in Malmberg-Penning traps makes them especially suitable for basic studies of plasma transport. It has long been known that electric and magnetic fields that break the cylindrical symmetry of these traps produce radial transport. Many researchers have studied this transport experimentally,[1–8] but connections to theory[9] have proved elusive.

Recently, Kabantsev and co-workers[10–12] have shown a remarkable connection between the damping of a trapped particle mode and the rate of asymmetry-induced radial expansion of the plasma. The damping of the trapped particle mode is produced by collisions that move particles from an axially trapped population to a population of particles that can move across the length of the device. Because this scattering from a trapped to untrapped state is relatively strong at the low collisionalities characteristic of most Malmberg-Penning traps, these results suggest that trapped particle effects play a dominate role in asymmetry-induced radial transport. Although most of their reported data uses a symmetric squeeze voltage applied to the center of the machine to produce the trapped particle distribution, they also present evidence that even weak axial variations in the magnetic field can produce trapped particles via the mirror effect. When a magnetic peak of approximately $\delta B/B_0 \approx 10^{-3}$ was removed from the central region of their plasma, the background transport decreased by a factor of 5. The identification of magnetic trapping is further supported by experiments which are designed to enhance scattering from the trapped to the untrapped populations.[13]

It has been suggested[12] that trapped particle effects might also help explain the discrepancies we observe between our transport experiments[7] and a quasilinear transport theory.[9] The key idea of this theory is that the radial transport is dominated by particles with an axial velocity that places them in resonance with the field asymmetry. These particles undergo large radial excursions until they are scattered out of resonance by collisions. The solenoid-produced axial magnetic field in our experiment, however, has a gentle rise in the field ($\delta B/B_0 \approx 4 \times 10^{-3}$) which could axially trap particles with low v_z and keep them from executing the assumed bounce motion between the ends of the trap. If the scattering from trapped to untrapped populations is faster than the scattering out of resonance, these trapped particles might play a key role in asymmetry-induced transport.

To test this idea, we have installed three additional magnetic field coils on our device to vary the axial field dependence and have examined the effect of these adjustments on the radial flux resonances we typically observe.[7] Making the magnetic field as uniform as possible reduces $\beta \equiv \delta B/B_0$ by a factor of 5.9, but this produces negligible change in the transport, in marked contrast to the observations of Kabantsev and co-workers. The coils are also used to increase the axial field variation. Although the transport shows some variation at these higher β levels, the variations cannot be simply explained in terms of trapped particles.

II. EXPERIMENTAL DEVICE

Our experiments are performed in a modified Malmberg-Penning trap in which the plasma has been replaced by a biased wire and the transport of low density test particles is studied. The rational for this design has been discussed in detail elsewhere.[7] Briefly stated, this design avoids previously encountered complications produced by collective effects and allows for simple tests of the transport physics.

The trap design is shown in Fig. 1. The axial magnetic field and negatively biased end cylinders of the standard trap design are retained, but the plasma is replaced by a thin

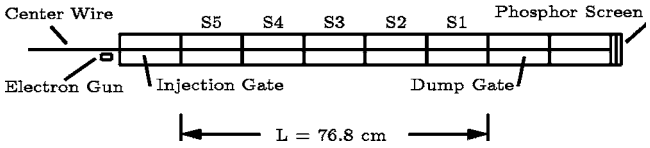

FIG. 1. Schematic of the Occidental College Trap. The usual plasma column is replaced by a biased wire to produce the basic dynamical motions in low density electrons injected from an off-axis gun. The low density and high temperature of the injected electrons largely eliminate collective modifications of the vacuum asymmetry potential. The five cylinders (labeled S1–S5) are divided azimuthally into eight sectors each.

biased wire (radius $a=0.007$ in.) suspended along the axis of the trap. This wire provides a radial electric field to replace the field normally produced by the plasma column and allows low density electrons injected into the device to have the same zeroth-order dynamical motions as those in a typical non-neutral plasma (axial bounce and azimuthal $E\times B$ drift motions). For these experiments the center wire bias $\phi_{cw}=-77.5$ V. The entire confinement region is sectored (five cylinders, labeled S1–S5 in Fig. 1, with eight azimuthal divisions each). For these experiments, we apply a known asymmetry by selecting the amplitude and phase of the voltages applied to each sector to produce a helical standing wave of the form

$$\phi(r,\theta,z,t)=\phi_W\frac{r}{R}\cos\left(\frac{n\pi z}{L}\right)\cos(l\theta-\omega t), \tag{1}$$

where ϕ_W is the asymmetry potential at the wall (typically 0.2 V), R is the wall radius (3.82 cm), L is the length of the confinement region (76.8 cm), n and l are the axial and azimuthal Fourier mode numbers, respectively, and here z is measured from one end of the confinement region. For these experiments $n=l=1$. The relative phases of the applied voltages are adjusted so that the asymmetry rotates in the same direction as the zeroth-order azimuthal $E\times B$ drift.

The details of our magnetic solenoid are shown in Fig. 2. A large bore (14.125 in. in diameter) aluminum coil form is wound with eight layers of 0.157×0.310 in. rectangular cross-section copper magnet wire. To maintain field uniformity over as large a volume as possible, eight additional layers are added to each end. The solenoid produces a maximum steady-state field of 607 G, but for these experiments $B=362$ G. Cancellation of the earth's magnetic field and fine alignment of the trap electrodes and the solenoid axis is obtained through the use of two sets of "bent head" rectangular field coils (not shown).[14] The adjustment of the axial field

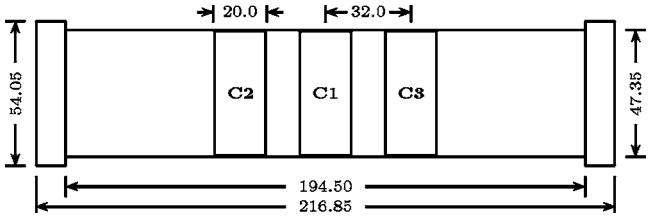

FIG. 2. Schematic of magnetic field coils. The addition of shim coils C1, C2, and C3 allows adjustment of the axial magnetic field variation. Dimensions are in centimeters.

variation required for this experiment is provided by three independent shim coils (labeled C1, C2, and C3) positioned symmetrically around the solenoid's midpoint as shown. These consist of 100 turns of 18 gauge wire wound on the topmost layer of the solenoid. The trap is positioned along the axis of the solenoid and the left edge of cylinder S3 is at the solenoid center.

The remaining features of the trap have been discussed in detail elsewhere.[7,15,16] Electrons injected into the trap from an off-axis gun are quickly dispersed into an annular distribution. At a chosen time (here, 1600 ms after injection), the asymmetries are switched on for a period of time δt (here, 100 ms) and then switched off. At the end of the experiment cycle, the electrons are dumped axially onto a phosphor screen and the resulting image is digitized using a 512×512 pixel charge-coupled device camera. A radial cut through this image gives the density profile $n_0(r)$ of the electrons. Calibration is provided by a measurement of the total charge being dumped. Profiles are taken both with the asymmetry on and off, and the resulting change in density $\delta n_0(r)$ is obtained. The background transport is typically small compared to the induced transport and is subtracted off. If the asymmetry amplitude is small enough and the asymmetry pulse length δt short enough, then $\delta n_0(r)$ will increase linearly in time.[5] We may then approximate $dn_0/dt\simeq\delta n_0(r)/\delta t$ and calculate the radial particle flux $\Gamma(r)$ (assuming $\Gamma(r=a)=0$):

$$\Gamma(r)=-\frac{1}{r}\int_a^r r'dr'\frac{dn_0}{dt}(r'). \tag{2}$$

Here a is the radius of the central wire. The entire experiment is then repeated for a series of asymmetry frequencies and the resulting flux vs radius and frequency data saved for analysis.

III. EXPERIMENTAL RESULTS

Our first experiment involves minimizing the axial magnetic field variations of the main solenoid and noting the change in the transport. Fig. 3 shows the calculated field variation $\delta B\equiv B(z)-B_0$ for three field coil configurations: the main solenoid alone, the solenoid along with shim coil C1 adjusted so that $\delta B\approx0$ at the solenoid center, and the solenoid along with the three shim coils adjusted so as to minimize δB overall. Here $B_0\approx371$ G is a constant subtracted to emphasize the variations in B and, in Fig. 3, z is measured from the center of the solenoid. The current in shim coils C2 and C3 is the same so the field is even with z. Note that these changes effect not only the maximum value of B but also the location of this maximum field (and, thus, the presumed mirror reflection point). To compare these cases, we define β as the difference between the maximum and minimum values of $\delta B/B_0$ for $z\leqslant46$ cm (corresponding to the end of the confinement region at the right edge of S1). Thus, the solenoid-only case has $\beta=0.435\%$ with the maximum field occurring at $z_{max}=0$ and the minimum at $z_{min}=46$ cm. With C1 added, we have $\beta=0.417\%$ but now $z_{max}=31.5$ cm and $z_{min}=0$. When all three shim coils are used

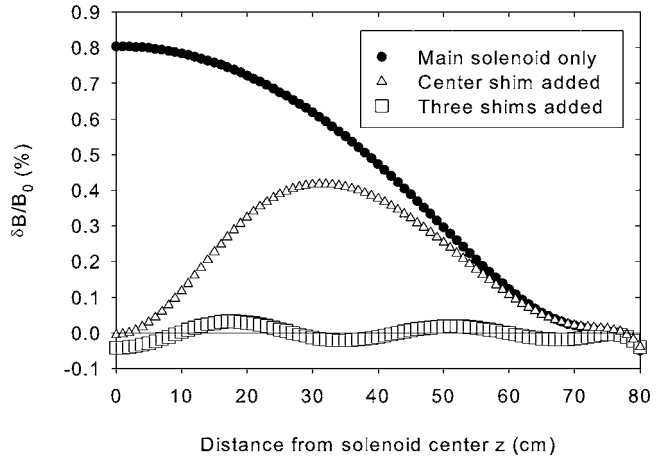

FIG. 3. Calculated magnetic field variations with axial position z. $z=0$ corresponds to the center of the solenoid. The three cases show the variation for the main solenoid alone, the solenoid along with shim coil C1 adjusted so that $\delta B \approx 0$ at $z=0$, and the solenoid along with the three shim coils adjusted so as to minimize δB overall. The symbol size for this last case gives an estimate of the maximum error due to winding imperfections and current measurement error.

$\beta=0.074\%$ with $z_{max}=18.0$ cm and $z_{min}=0$. This last case thus gives a reduction in β by a factor of 5.88 over the solenoid-only case.

We typically characterize the transport by a plot of radial particle flux versus asymmetry frequency with radial position as a parameter, as shown in Fig. 4. We display data taken for the solenoid-only case as well as the minimum β case using three shim coils. The data show negligible change in the transport. Not shown is the data for the case using only coil C1, but it also exhibits negligible change. Thus, neither reducing β nor changing the position of the field maximum has a significant effect on the transport for these β levels.

We can also use the shim coils to increase the variation in B as shown in Fig. 5. For these cases the current in C1 is run opposite to the current in C2 and C3 to create a field that

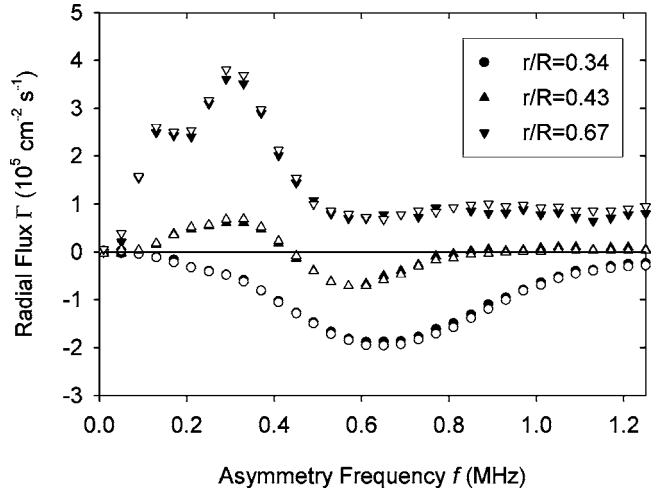

FIG. 4. Measured radial particle flux vs. asymmetry frequency with radial position as a parameter. The filled symbols show data taken using the main solenoid only while the open symbols show data taken with magnetic variations minimized through use of the three shim coils (cf. Fig. 3). The difference is negligible.

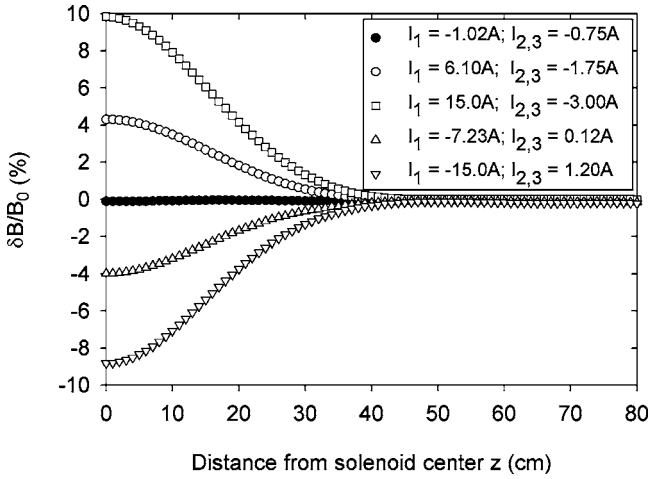

FIG. 5. Magnetic field variation with z when shim coils are used to increase β and produce a field that is more peaked at $z=0$. For comparison, the filled circles show the minimum β case of Fig. 3.

is more peaked at $z=0$. For these experiments, we define $\beta \equiv (\delta B(z=0) - \delta B(z=46))/B_0$, so β can be positive or negative. Positive β would produce trapped particle distributions at the ends of the machine whereas negative β would produce trapped particles in the center.

These stronger variations in the magnetic field produce larger changes in the transport, as shown in Fig. 6. The upper

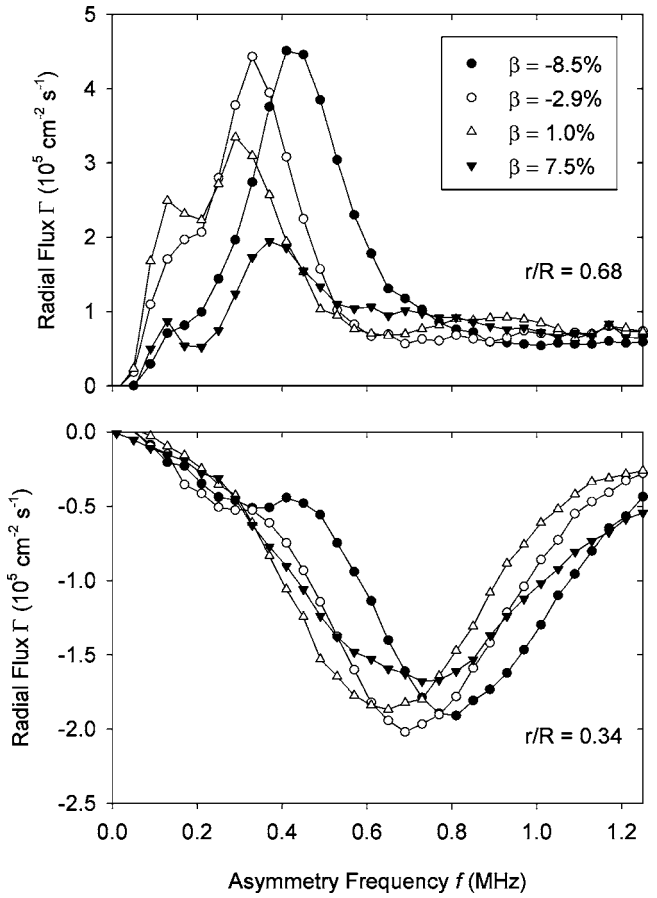

FIG. 6. Representative changes to the transport produced by larger β variations. Flux peaks are shown at two representative radii.

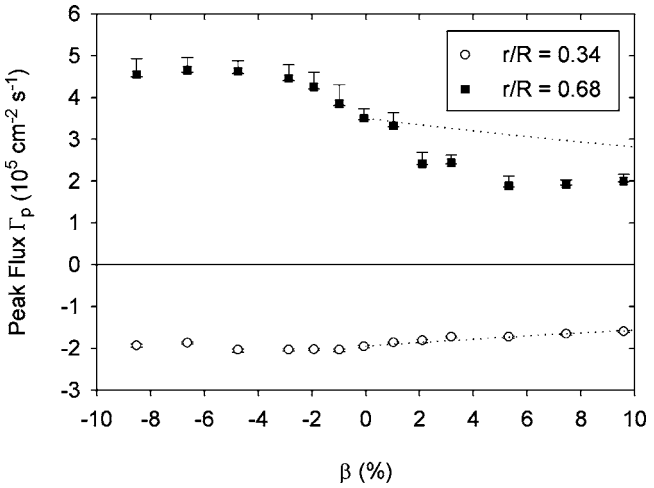

FIG. 7. The peak radial flux Γ_p vs β. Negative β corresponds to negative δB at $z=0$ (cf. Fig. 5). The dotted lines are the prediction of the model given in Sec. IV normalized to match the data at $\beta=0$.

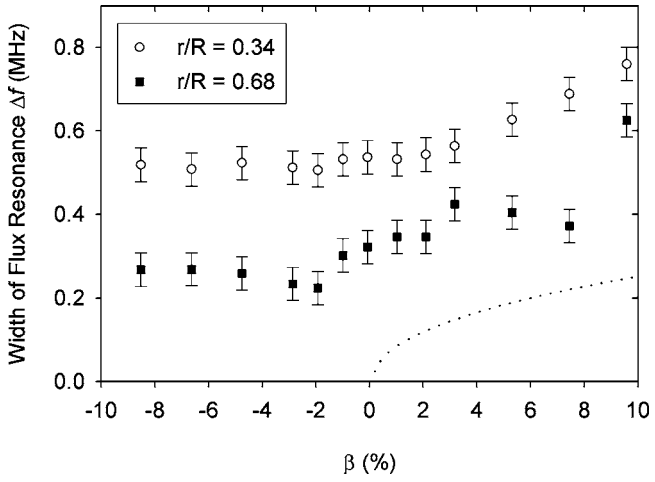

FIG. 9. The width of the flux resonance Δf vs β. The dotted line is the prediction of the model given in Sec. IV. Here the prediction is independent of radius.

and lower plots show radial flux versus asymmetry frequency for $r/R=0.68$ and $r/R=0.34$, respectively, with β as a parameter. To characterize the changes in the transport, we extract from plots like Fig. 6 three quantities: the peak flux Γ_p (i.e., the maximum or minimum value of the flux), the peak frequency f_p (i.e., the frequency at which Γ_p occurs), and the width of the flux peak Δf (i.e., the full width at half-maximum (FWHM) of the Γ vs. f plots). These results are given in Figs. 7–9. The error bars are estimates of the uncertainty due to finite number of frequencies used.

Variations in the peak flux are most pronounced at the larger radius. Positive β reduces the magnitude of Γ_p whereas negative β increases it. The variations appear to saturate within our β range at about ±40% of the $\beta=0$ value for the $r/R=0.68$ case. Significant variations in the peak frequency, in contrast, appear at both larger and smaller radii, with increases of 20%–40% of the $\beta=0$ value. The peak frequency increases with both positive and negative β in a fairly symmetrical way. The width of the flux peak, Δf, also varies at both larger and smaller radii, but is asymmetrical with the sign of β, increasing most significantly (40%–90%) only with positive β.

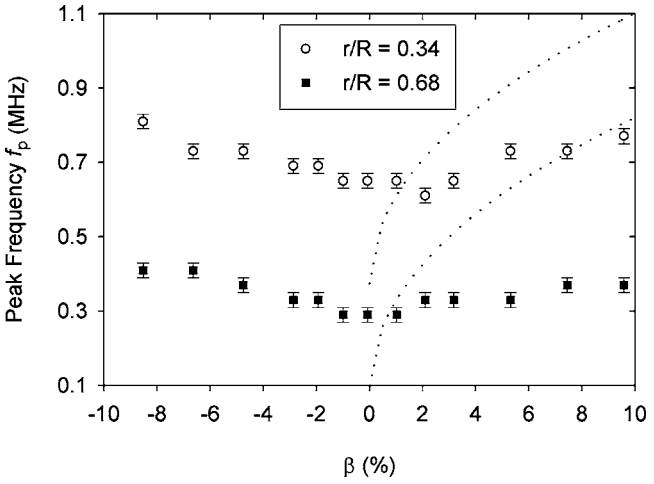

FIG. 8. The peak frequency f_p vs β. The dotted lines are the prediction of the model given in Sec. IV.

IV. DISCUSSION

We now compare these results with a simple model combining resonant particle effects with the current understanding of trapped particle transport. We start with the notion that particles moving in resonance with the asymmetry have the largest radial excursions. These particles have axial velocities v_{res} satisfying

$$f - lf_R - \frac{n}{2L_{\mathrm{res}}} v_{\mathrm{res}} = 0, \tag{3}$$

where f_R is the $E\times B$ drift rotation frequency and L_{res} is the length of the particle's axial excursion, which now may be different from the trap length due to mirroring. As the asymmetry frequency f is varied, the resonant velocity v_{res} will sweep through a range of values and the transport flux $\Gamma(f)$ will reflect the distribution of particles participating in the transport. Transport occurs when collisions scatter particles out of resonance.

When an axial variation in the magnetic field is present, the particle distribution is divided into two populations: those that are trapped axially (i.e., reflected by the magnetic mirror) and those that are not trapped. A separatrix in velocity space separates these two populations. Even small velocity scattering can cause particles near the separatrix to move from the trapped to untrapped population. If this is the dominant scattering process, then particles near the separatrix will dominate the transport.

We expect, then, the transport to be proportional to the value of the distribution function on the separatrix between trapped and untrapped populations. This separatrix is given by[17]

$$v_\perp^2 = \frac{1}{\beta}\left(v_z^2 + \frac{2e\Delta\phi}{m}\right), \tag{4}$$

where $\Delta\phi$ is the potential difference along a field line produced by the axial variation of the magnetic field. For an isotropic Maxwellian distribution, the density along this separatrix is proportional to

$$F(v_z) = \left[\frac{1}{\beta}\left(\frac{v_z^2}{\bar{v}^2} + \frac{2e\Delta\phi}{kT}\right)\right]^{1/2} \exp\left(-\frac{\beta+1}{\beta}\frac{v_z^2}{2\bar{v}^2} - \frac{e\Delta\phi}{\beta kT}\right). \tag{5}$$

This function peaks at $v_z = v_p$ where

$$v_p = \bar{v}\left[\frac{\beta}{1+\beta} - \frac{2e\Delta\phi}{kT}\right]^{1/2} \tag{6}$$

and has a FWHM of

$$\Delta v = \bar{v}\left[\left(\frac{3.69\beta}{1+\beta} - \frac{2e\Delta\phi}{kT}\right)^{1/2} - \left(\frac{0.10\beta}{1+\beta} - \frac{2e\Delta\phi}{kT}\right)^{1/2}\right]. \tag{7}$$

Using these results in Eq. (3), the measured flux resonances should peak at frequency $f_p = lf_R + nv_p/2L_{\text{res}}$ and have a width $\Delta f = n\Delta v/2L_{\text{res}}$. Plugging into Eq. (5), we find the peak flux

$$\Gamma_p \propto F(v_p) \propto (1+\beta)^{-1/2}\exp\left(\frac{e\Delta\phi}{kT}\right). \tag{8}$$

To evaluate these expressions we need to determine $\Delta\phi$ and L_{res}. In our trap where the electron density is low, the potential as a function of radius is given by the vacuum expression

$$\phi(r) = \phi_{\text{cw}}\frac{\ln(R/r)}{\ln(R/a)} \tag{9}$$

and $\Delta\phi$ can be shown to be

$$\Delta\phi = \frac{\phi_{cw}}{2\ln(R/a)}\ln(1+\beta) \tag{10}$$

independent of radius (assuming B is uniform with r at the ends of the mirror). This in turn means that $f_p - lf_R$, Δf, and $F(v_p)$ are also independent of radius.

It remains to determine L_{res}. For positive β, this is the distance between the ends of the confinement region and the field peak. Since the field peak is not equidistant from the two ends, we take the average of these two distances and use $L_{\text{res}} = 38.4$ cm.

Our model does not seem to be meaningful for negative β. A trapped particle starting at $z=0$ will mirror reflect at the ends of the trap, but the reflection point is the same if the particle does not mirror reflect since for this case the end confining potentials produce the reflection. Thus there is no difference in axial excursion between trapped and untrapped particles and separatrix crossing cannot lead to transport.

The model predictions for positive β are shown by the dotted lines in Figs. 7–9. For Fig. 7, we have normalized the prediction of Eq. (8) to match the data at $\beta=0$. In Fig. 8, the upper line corresponds to $r/R=0.34$ and the lower line to $r/R=0.68$. Only one line is shown in Fig. 9 since the predicted Δf is independent of radius. With the exception of $\Gamma_p(r/R=0.34)$, the fit to the data is poor.

We note that the model assumes that the parallel and perpendicular velocity distributions are Maxwellian and equilibrated, an assumption we are unable to check in the current experiments because we have no diagnostic for $v_\perp$. The low electron-electron collision rate in our device ($\nu_{\text{ee}} \approx 0.25\ \text{s}^{-1}$) would not allow for equilibration during the 1.6 s confinement period, so the $v_\perp$ distribution would be substantially the same as it was at injection. Absence of large $v_\perp$ values could then explain the null result of Fig. 4. Some trapping would occur with only partial isotropization, particularly at the higher β levels, but without complete velocity distribution measurements such trapping effects cannot be quantified. The variation of our transport characteristics for negative beta (where transport due to separatrix crossing cannot occur), however, suggests that other transport processes are operative and significant.

V. CONCLUSION

We have measured the dependence of characteristic radial transport resonances on axial variations in magnetic field. Reducing the small variations in our solenoid by a factor of 5.9 has negligible effect on the transport. For β variations up to 10%, variations of 20%–90% are seen in the transport characteristics. We are unable to explain these results in terms of a simple model of trapped particle transport.

ACKNOWLEDGMENTS

This work was supported by U.S. Department of Energy Grant No. DE-FG03-98ER54457 and NSF/DOE PHY0354979.

[1] D. L. Eggleston, T. M. O'Neil, and J. H. Malmberg, Phys. Rev. Lett. **53**, 982 (1984).
[2] J. Notte and J. Fajans, Phys. Plasmas **1**, 1123 (1994).
[3] X.-P. Huang, F. Anderegg, E. M. Hollman, C. F. Driscoll, and T. M. O'Neil, Phys. Rev. Lett. **78**, 875 (1997).
[4] J. M. Kriesel and C. F. Driscoll, Phys. Rev. Lett. **85**, 2510 (2000).
[5] D. L. Eggleston and B. Carrillo, Phys. Plasmas **9**, 786 (2002).
[6] E. Gilson and J. Fajans, Phys. Rev. Lett. **90**, 015001, (2003).
[7] D. L. Eggleston and B. Carrillo, Phys. Plasmas **10**, 1308 (2003).
[8] J. R. Danielson and C. M. Surko, Phys. Rev. Lett. **94**, 035001 (2005).
[9] D. L. Eggleston and T. M. O'Neil, Phys. Plasmas **6**, 2699 (1999).
[10] A. A. Kabantsev and C. F. Driscoll, Phys. Rev. Lett. **89**, 245001 (2002).
[11] A. A. Kabantsev, J. H. Yu, R. B. Lynch, and C. F. Driscoll, Phys. Plasmas **10**, 1628 (2003).
[12] C. F. Driscoll, A. A. Kabantsev, T. J. Hilsabeck, and T. M. O'Neil, in *Non-Neutral Plasma Physics V*, edited by M. Schauer, T. Mitchell, and R. Nebel (American Institute of Physics, Melville, New York, 2003), p. 3.
[13] A. A. Kabantsev and C. F. Driscoll, Rev. Sci. Instrum. **74**, 1925 (2002).
[14] O. Klemperer and M. E. Barnett, *Electron Optics*, 3rd. ed. (Cambridge University Press, New York, 1971), pp. 166 and 167.
[15] D. L. Eggleston, Phys. Plasmas **4**, 1196 (1997).
[16] D. L. Eggleston, Phys. Plasmas **1**, 3850 (1994).
[17] J. Fajans, Phys. Plasmas **10**, 1209 (2003).